Heliyon 9 (2023) e22099

Contents lists available at ScienceDirect

Heliyon

journal homepage: www.cell.com/heliyon

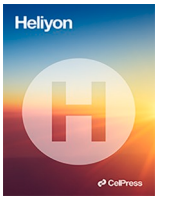

One-pot synthesized copper-imidazole-2-carboxaldehyde complex material with oxidase-like activity for the colorimetric detection of glutathione and ascorbic acid

Jia-Xin Li, Jia-Li Wang, Tong-Qing Chai, Feng-Qing Yang *

School of Chemistry and Chemical Engineering, Chongqing University, Chongqing, 401331, PR China

ARTICLE INFO

Keywords:
Copper-imidazole-2-carboxaldehyde
Oxidase-like activity
Ascorbic acid
Glutathione

ABSTRACT

Due to the copper (Cu) active sites, its complexes with oxidase-like activity have superior catalytic properties, which can catalyze a series of specific substrates like 3,3′,5,5′-tetramethylbenzidine (TMB), producing colorimetric reactions for the detection of different reducing small-molecule compounds. Attribute to the competitive coordination effects between water molecules and central Cu ions, most of the Cu complexes can hardly be used in the pure aqueous reaction system. In this study, a Cu-based material (Cu-imidazole-2-carboxaldehyde, Cu-ICA) was prepared using copper ions and ICA through a one-step process in the water solution. After the morphology of the material being characterized, the mimetic enzyme behavior of the Cu-ICA was demonstrated through the TMB oxidation. Compared to the other reported oxidase-like mimics, Cu-ICA has better aqueous stability and oxidase-like activity, and shows a higher v_{max}. Furthermore, basing on the oxidase-like activity of Cu-ICA, a colorimetric method was developed for the ascorbic acid and glutathione detections with linear ranges of 0.5–5 μM and 0.5–4 μM, and limit of detection of 0.1304 μM and 0.097 μM, respectively. Owing to its excellent aqueous stability and oxidase-like activity, Cu-ICA has bright application prospects in the analysis of reducing small-molecule compounds.

1. Introduction

As an important biocatalyst with excellent catalytic activity and high selectivity, oxidase has been usually applied in the pollutant treatment [1,2], diagnostic kits [3], and biosensor development [4]. However, there are several shortcomings in the practical applications of natural oxidase [5–8], including high preparation and purification cost, low operational stability and yield, poor stability in harsh environments, and difficulties in recycling and reusing. Therefore, the development of alternatives to oxidase has become a focus of increasing attention. To date, various oxidase mimics, such as metal-organic frameworks [9,10], covalent organic frameworks [11], single-atom catalysts [12,13], metals and metal oxides [14], carbon-based nanomaterials [15] and transition metal complex [16], have been successfully prepared and applied in the environmental monitoring, biomedical and chemical analysis.

Abbreviations: **AA**, ascorbic acid; **EDX**, energy dispersive X-ray spectroscopy; **Fmoc**, fluorenylmethyloxycarbonyl; **FT-IR**, Fourier transform infrared spectroscopy; **GSH**, glutathione; **His**, histidine; **ICA**, imidazole-2-carboxaldehyde; **IPA**, isopropyl alcohol; **LOD**, limit of detection; **SEM**, scanning electron microscope; **TMB**, 3,3′,5,5′-tetramethylbenzidine; **XPS**, X-ray photoelectron spectroscopy; **XRD**, X-ray diffraction.

* Corresponding author. School of Chemistry and Chemical Engineering, Chongqing University, Chongqing, 401331, PR China.
E-mail address: fengqingyang@cqu.edu.cn (F.-Q. Yang).

https://doi.org/10.1016/j.heliyon.2023.e22099
Received 21 September 2023; Received in revised form 25 October 2023; Accepted 3 November 2023
Available online 4 November 2023

Transition metal elements, including copper (Cu), cobalt (Co), iron (Fe), and manganese (Mn), are essential for normal biological functions, which usually paly part in electron transfer reactions [17]. As functional and structural models for metalloenzymes with oxidase activity, the transition metal complexes have been extensively studied [18]. For example, PCN-224-Mn [19] was synthesized by Mn ions modifying porphyrin metal-organic framework, which exhibits oxidase-like activity that can catalyze the 3,3′,5,5′-tetramethylbenzidine (TMB) oxidation. Besides, Zhang et al. [20] reported phenanthroline (Fe (III)-L_3) or Fe (III) bipyridyl complexes have oxidase-like activity that can be used for sensitively colorimetric detection of glutathione (GSH) using TMB as the chromogenic substrate. Cu is presented in many native metalloproteins and plays the basic biological role of copper metalloenzymes, therefore, significant attentions have been paid to the oxidase-like property of Cu complex during the past decades. In particular, several oxidase-like Cu enzyme mimics have been applied in the catalysis of oxidation processes of different substrates, including amines, carbohydrates, and phenols, etc [21]. Early in 2001, Cu (II) complexes with aminocarbohydrate β-ketoenaminic as ligands are synthesized, show great catalytic oxidation activity in catalyzing catechol oxidation [22]. Besides, Cu (II) complexes with 4,6-di (*tert*-butyl)-2-aminophenoland 2-anilino-4,6-di (*tert*-butyl) phenol [23] were prepared as antimicrobial agents based on their strong oxidase-like activity. In addition, Xu et al. [24] report a self-assembled complex of Cu (II) with fluorenylmethyloxycarbonyl (Fmoc)-modified amino acid and nucleotides, which can catalyze the oxidation of catechol to innocuous substance attributed to the catechol oxidase-like Cu-cluster active sites.

In 2022, Wang et al. [25] first reported a novel type of nanomaterial denoted as I-Cu, which was prepared by combining Cu^{2+} with the N atoms in the imidazole to form Cu–N coordinated bond. I-Cu has very good laccase-like activity due to the N–Cu coordinated environment between the imidazole and Cu^{2+} in their active site, which exhibits bright prospect in the detection of dopamine and oxidation of phenolic pollutants. Furthermore, early in 1999, Barszcz et al. [26] investigated the crystal and molecular structures of eight-coordinate (CuN_4O_4) and six-coordinate (CuN_4O_2) Cu (II) complexes with 4-methyl-5-imidazole-carboxaldehyde or 1-benzyl-2-hydroxymethylimidazole, respectively. The results showed that Cu can coordinate with the O atoms on the aldehyde group in imidazole derivatives. Therefore, in this study, the imidazole-2-carboxaldehyde (ICA), which contains nitrogen atoms on the imidazole group and oxygen atoms on the aldehyde group that can be combined with Cu ions, was introduced as a ligand. Then, an active Cu artificial oxidase Cu-ICA was designed and synthesized through a one-step approach. The Cu-ICA can catalyze the TMB oxidation without the addition of H_2O_2. The oxidase-like activity of Cu-ICA was used in colorimetric detection of GSH and ascorbic acid (AA) after the reaction conditions being carefully investigated. The results indicate that the method has a high sensitivity and selectivity. This is the first time that Cu (II) was combined with ICA to prepare a complex material with excellent oxidase activity, which was further applied in the colorimetric detection of small-molecule compounds.

2. Materials and methods

2.1. Materials and apparatus

The information of materials and apparatus is shown in the Electronic Supplementary Materials.

2.2. Preparation of Cu-ICA

The Cu-ICA was synthesized through a facile one-step process. In brief, 60 mg of ICA was heated at 60 °C and then dissolved by ultrasound in 4 mL of water, 4 mg of $CuSO_4{\cdot}5H_2O$ was dissolved in 4 mL of water to obtain 1 mg/mL of Cu^{2+} solution. Mixed 4 mL of each reactant solution in room temperature (about 25 °C), and then got a kind of pale brown suspension immediately. The obtained product is the Cu-ICA suspension.

Furthermore, to investigate the oxidase-like activity of Cu-ICA in different raw material ratio, the mass ratio of ICA to $CuSO_4{\cdot}5H_2O$ (1 mg/mL) was investigated at 5, 10, 15, 20, and 25. On the other hand, the synthesis time was investigated by changing the incubation time (0, 5, 10, 20 and 30 min) during the synthesis of Cu-ICA. The optimal ratio and synthesis time were used for the further experiments.

2.3. Oxidase-like activity of Cu-ICA

TMB was used as the substrate molecule to evaluate the oxidase-like activity of Cu-ICA through colorimetric analysis. Firstly, 50 μL of $CuSO_4{\cdot}5H_2O$ (1 mg/mL), 50 μL of ICA (15 mg/mL), and 300 μL of buffer solution (NaAc/HAc, pH 4.0) was added into a 0.5-mL centrifuge tube, which was mixed at room temperature (about 25 °C). Then, 100 μL of TMB (final concentration of 2 mM) was added into the mixture and reacted at 30 °C for 5 min. Lastly, filtered the solution through a 0.22 μm pore membrane, the absorbance of ox-TMB at 658 nm was obtained by the UV-Vis spectrophotometer.

2.4. Kinetic analysis and mechanism investigation

The kinetics of catalysis of TMB was studied through measuring the absorption at 658 nm with a time-scan mode. The reaction solution with a total volume of 500 μL was incubated under optimal conditions, which contains 50 μL of $CuSO_4{\cdot}5H_2O$ (1 mg/mL), 50 μL of ICA (15 mg/mL), 300 μL of buffer solution (NaAc/HAc, pH 4.0) and 100 μL of TMB with different concentrations (final concentrations of 0.8, 1.0, 1.2, 1.6, 2.0, 2.4, 2.8, 3.2, 3.6, and 4.0 mM). After the reaction for 4 min, filtered the solution through a 0.22 μm pore membrane. The absorption at 658 nm of the reaction mixture was measured immediately. According to the Michaelis-Menten

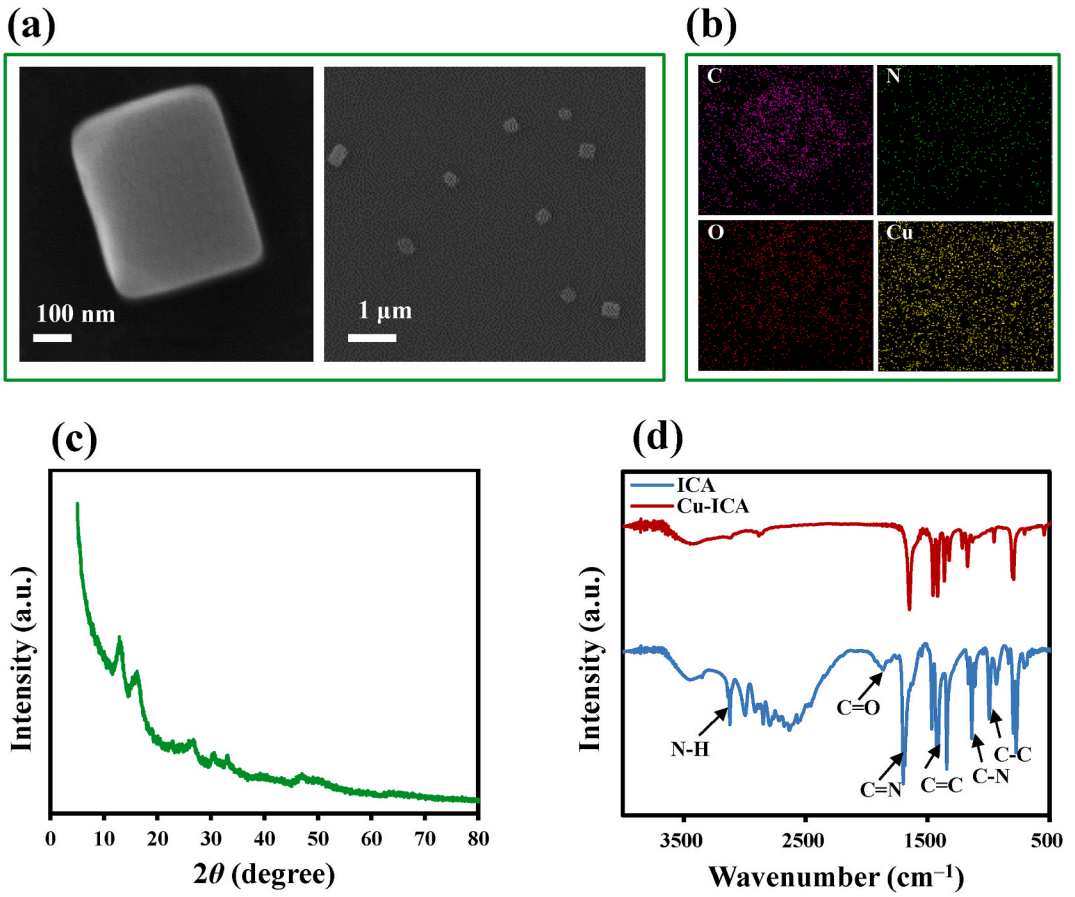

Fig. 1. (**a**) SEM images of Cu-ICA nanoparticles; (**b**) EDS mapping of Cu-ICA nanoparticles; (**c**) XRD analysis of Cu-ICA; (**d**) FT-IR spectral of Cu-ICA and ICA.

equation (1), the kinetic parameters were obtained.

$$\nu = \frac{\nu_{max} \times [S]}{K_m + [S]} \tag{1}$$

where ν and ν_{max} are the initial and maximal reaction velocity, respectively, K_m is the Michaelis constant, and [S] is the substrate (TMB) concentration.

In addition, the active species-scavenging experiments were performed to investigate the mode of action of Cu-ICA's oxidase-like activity. Histidine (His), isopropyl alcohol (IPA), and *p*-benzoquinone, which are served as the scavengers of singlet oxygen ($^1O_2$), hydroxyl radicals (•OH), and superoxide radicals (O_2^-), were added to the Cu-ICA and TMB mixed solution, and then incubated for 4 min, respectively. Lastly, the absorbance spectra of the reaction mixtures were recorded.

2.5. Determination of GSH and AA by Cu-ICA based colorimetric method

Typically, for the analysis of GSH and AA, 50 μL of $CuSO_4 \cdot 5H_2O$ (1 mg/mL), 50 μL of ICA (15 mg/mL), and 250 μL of buffer solution (NaAc/HAc, pH 4.0) were mixed in a 0.5-mL centrifuge tube. Then, 50 μL of GSH or AA with different concentrations were introduced into the solutions, respectively. Finally, 100 μL of TMB (final concentration of 3.2 mM) as chromogenic substrate was introduced, the total volume of the mixture was 500 μL. After incubating at 45 °C for 4 min and filtering the reaction solution through a 0.22 μm pore membrane, the absorption at 658 nm was measured.

In addition, to investigate the effects of interfering compounds on the detection of GSH and AA, the relevant interference experiments were performed. The interference solutions (final concentration of 400 μM), which include AA (final concentration of 4 μM) or GSH (final concentration of 4 μM), was measured and compared, respectively. The interferences are Lys, Arg, glucose, lactose, fructose, Ca^{2+}, Mg^{2+}, K^+, and Na^+.

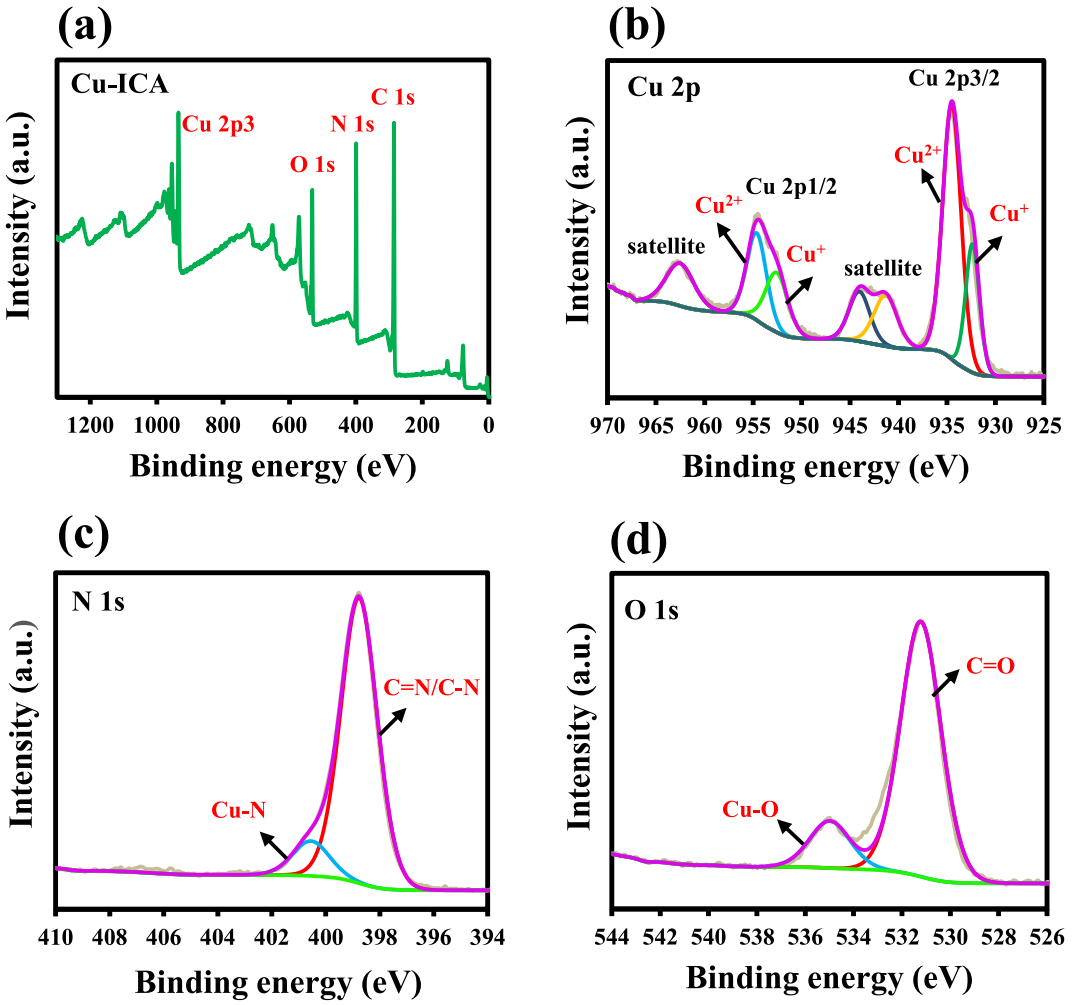

Fig. 2. XPS analysis of Cu-ICA: (**a**) survey spectrum, (**b**) Cu 2p, (**c**) N 1s, (**d**) O1s.

2.6. Real sample analysis

In brief, the various reactants with a total volume of 500 mL, including 50 μL of $CuSO_4{\cdot}5H_2O$ (1 mg/mL), 50 μL of ICA (15 mg/mL), 250 μL of buffer solution (NaAc/HAc, pH 4.0), 50 μL of sample solution, and 100 μL of TMB (final concentration of 3.2 mM), were mixed uniformly. After being incubated at 45 °C for 4 min and filtered through a 0.22 μm pore membrane, the absorbance of the mixture at 658 nm was obtained.

The sample solution preparation process was as follows. The commercially available GSH tablet (0.1491 g) and AA tablet (0.1180 g) were ground into powder and dissolved 0.0149 g and 0.0118 g of them in 8 mL of ultrapure water, respectively. After that, extracted the active ingredients by ultrasound for 30 min, and then diluted the mother solution for 20 times to make the real sample solution.

3. Results and discussion

3.1. Characterization of the materials

The scanning electron microscopy (SEM) was used to characterize the morphology of the prepared materials. Fig. 1a indicates that the Cu-ICA has a regular rectangular structure and the particle width is about 400 nm. Furthermore, the particles contain C, N, O, and Cu elements according to the energy dispersive X-ray spectroscopy (EDX) images shown in Fig. 1b. To further characterize the crystal structure of Cu-ICA, X-ray diffraction (XRD) was performed and the result was shown in Fig. 1c. The Cu-ICA does not exhibit obvious and sharp diffraction peaks due to the incomplete crystallization effect, indicating the material is amorphous crystal. What's more, the Fourier transform infrared spectroscopy (FT-IR) of Cu-ICA was demonstrated in Fig. 1d. The band at 3127 cm^{-1}, which was disappeared in Cu-ICA, was assigned to N–H strength vibration of the ligand (ICA), obviously demonstrating the coordination of amino group of ICA with Cu. Meanwhile, the band at 1865 cm^{-1} was C═O strength vibration peak of a five-membered ring, its disappearance

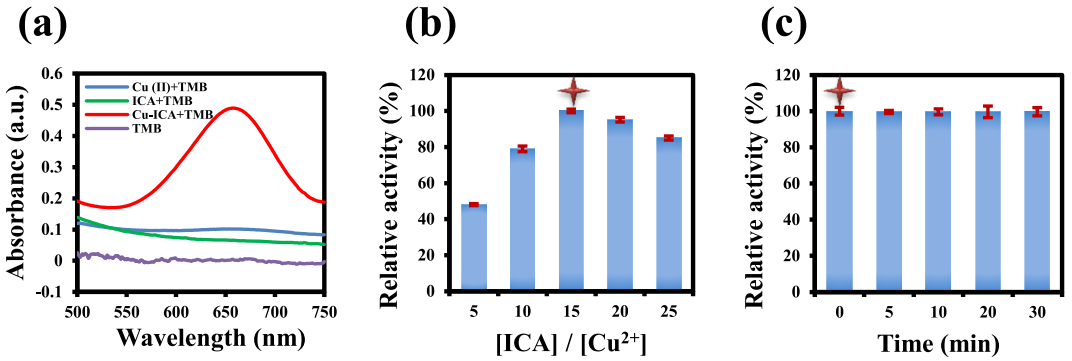

Fig. 3. (**a**) UV-Vis absorption spectra of 0.10 M of buffer solution (NaAc/HAc, pH 4.0) containing Cu (II) + TMB, ICA + TMB, Cu-ICA + TMB, and TMB; Effects of (**b**) the ratio of ICA to Cu (II) and (**c**) incubation time of synthesis on the oxidase-like activity of Cu-ICA.

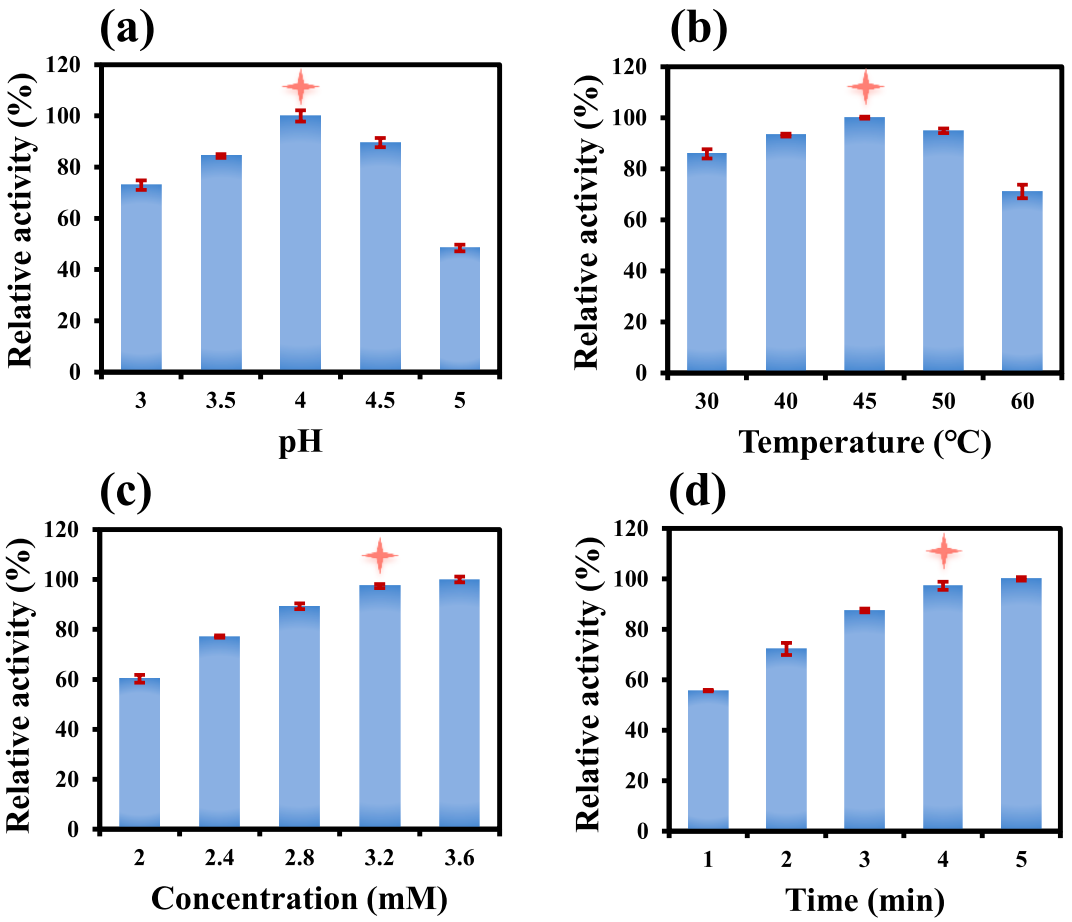

Fig. 4. Effects of (**a**) pH, (**b**) temperature, (**c**) final concentration of TMB, and (**d**) incubation time on the oxidase-like activity of Cu-ICA.

illustrated the coordination of carbonyl group with Cu. Besides, the absorption peaks of C–C, C–N, C═C, and C═N stretching vibrations were at 996, 1213, 1453 and 1647 cm^{-1}, respectively. The Cu-ICA retained the basic structure of ligand ICA.

The X-ray photoelectron spectroscopy (XPS) of Cu-ICA was measured to study its chemical compositions and chemical states. Fig. 2a displays the survey spectrum of pure Cu-ICA, which appears the peaks of Cu 2p, O 1s, N 1s, and C 1s. Fig. 2b displays the core-level and shake-up satellite (sat.) lines of Cu 2p. Fitting the Cu 2p spectrum, the Cu 2p3/2 and Cu 2p1/2 can split into two peaks. The peaks of 934.49 and 954.62 eV are assigned to the Cu 2p3/2 and Cu2p1/2 electrons of Cu^{2+}, respectively. The peaks of lower binding energy at 932.36 and 952.56 eV suggest the presence of Cu^{+}. Therefore, a fraction of Cu^{2+} was reduced, which may explain the high oxidase-like activity of Cu-ICA during the reaction. Furthermore, there are two peaks of N 1s (Fig. 2c) with binding energy of 398.8 and

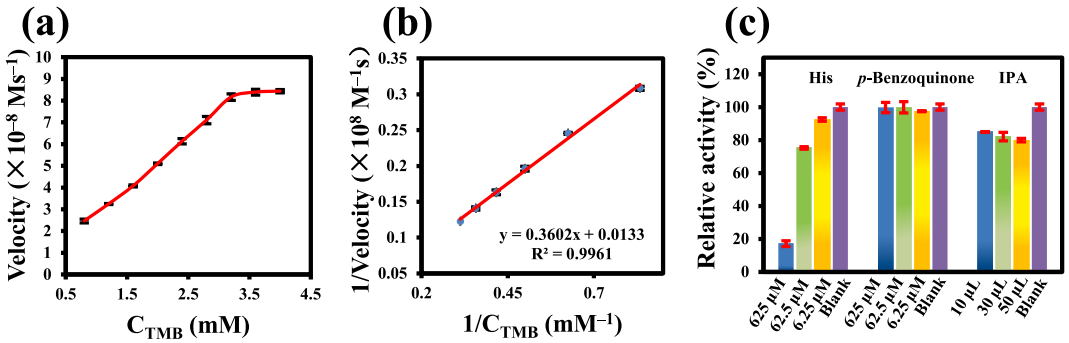

Fig. 5. (**a**) Michaelis-Menten equation under 1 mg/mL of Cu (II) and 15 mg/mL of ICA with varied final concentrations of TMB and (**b**) the corresponding double-reciprocal plots of Cu-ICA-catalyzed activity; (**c**) Effects of different active scavengers on the catalysis of TMB by Cu-ICA.

Table 1
Comparison of K_m and v_{max} of the Cu-ICA and reported oxidase-like mimics.

Catalysts	Substrate	K_m (mM)	$v_{max} \times 10^{-8}$ Ms^{-1}	Ref.
Ir NPs	TMB	0.280	13.650	[29]
Co_4S_3/Co $(OH)_2$HNTs	TMB	1.33	46.6	[30]
Mn_3O_4 NFs	TMB	13.2	1.35	[31]
Ni/Co-MOF	TMB	0.255	1.346	[32]
Cu-ICA	TMB	27.08	75.19	This work

400.5 eV that are attributed to the C═N/N–C and Cu–N, respectively, confirming the formation of Cu-ICA. Besides, in Fig. 2d, the two peaks in the O 1s spectrum prove the existence of Cu–O (534.68 eV) and C═O (531.28 eV). In addition, three characteristic peaks of the C 1s spectrum (Fig. S1) were observed at 284.7, 286.2, and 290.1 eV, which are attributed to the C═C/C–C, C═N, and C–N, respectively.

3.2. Oxidase-like activity of Cu-ICA

TMB can be oxidized into a color product in the presence of oxidase-like enzymes without the help of H_2O_2 [27], therefore, the oxidation of TMB was used as a probe to assess the oxidase-like activity of Cu-ICA. As shown in Fig. 3a, Cu-ICA can catalyze the oxidation of color developing substrate TMB to obtain the corresponding oxidation product, and there was an obvious absorption peak at 658 nm. However, the characteristic absorption peak was negligible when the reaction solution only contained $CuSO_4{\cdot}5H_2O$ or ICA or TMB, which verified the oxidase-like catalytic activity of Cu-ICA. Furthermore, the results displayed in Fig. 3b indicate that when the mass ratio of ICA (15 mg/mL) and $CuSO_4{\cdot}5H_2O$ (1 mg/mL) was 15:1, the Cu-ICA showed the best oxidase-like activity. In addition, as the results depicted in Fig. 3c, the incubation time of Cu-ICA synthesis had little influence on the oxidase-like activity of Cu-ICA.

The pH, temperature, incubation time, and TMB concentration may influence the oxidase-like activity of Cu-ICA. To obtain the optimal reaction conditions, the influencing factors on the oxidase-like activity of Cu-ICA were studied. As shown in Fig. 4a, under neutral or alkaline conditions, the oxidase-like catalytic activity of Cu-ICA decreased, and the best activity was obtained at pH 4.0. Moreover, the Cu-ICA kept relative stable in catalytic activity under the investigated temperature (30–60 °C), and the temperature dependent oxidase-like activity (Fig. 4b) indicates that the optimal temperature was 45 °C. In addition, as the results shown in Fig. 4c and d, the oxidase-like activity of Cu-ICA reached a saturation when the final concentration of TMB and incubation time were 3.2 mM and 4 min, respectively. In summary, the optimal reaction conditions for the analysis are as follows, pH 4.0, 45 °C, 3.2 mM of TMB (final concentration), and 4 min of incubation time.

3.3. Kinetic analysis and mechanism investigation

The kinetic study of Cu-ICA-catalyzed reaction was conducted through steady-state kinetics experiments. The results shown in Fig. 5a indicate the reaction velocity of TMB at varied final concentrations, and Fig. 5b shows the corresponding double-reciprocal plots. Results show that the catalytic activity of the synthesized Cu-ICA conformed to the Michaelis-Menten equation. The Michaelis-Menten constant (K_m) and maximal reaction velocity (v_{max}) were calculated to be 27.08 mM and 75.19 $\times$ 10^{-8} M s^{-1}, respectively, according to the Lineweaver-Burk double reciprocal curve. As an important indicator of the affinity between substrate and the enzyme, a lower value of K_m represents a higher affinity [28]. As collected in Table 1, the v_{max} of Cu-ICA is much higher than the other small-molecule and nanomaterials-based oxidase mimics, which indicates the superiority of Cu-ICA in oxidizing of TMB. As a ligand, ICA provides two atoms (N and O) to combine with the active sites (Cu^{2+}), leading to the Cu-ICA complex contains more active sites when ligands are quantitative. Furthermore, the lamellar structure of Cu-ICA enables it has a relatively higher specific surface area as compared with the bulk material, thus accelerating the reaction rate. Moreover, the K_m value of Cu-ICA is 27.08 mM using TMB

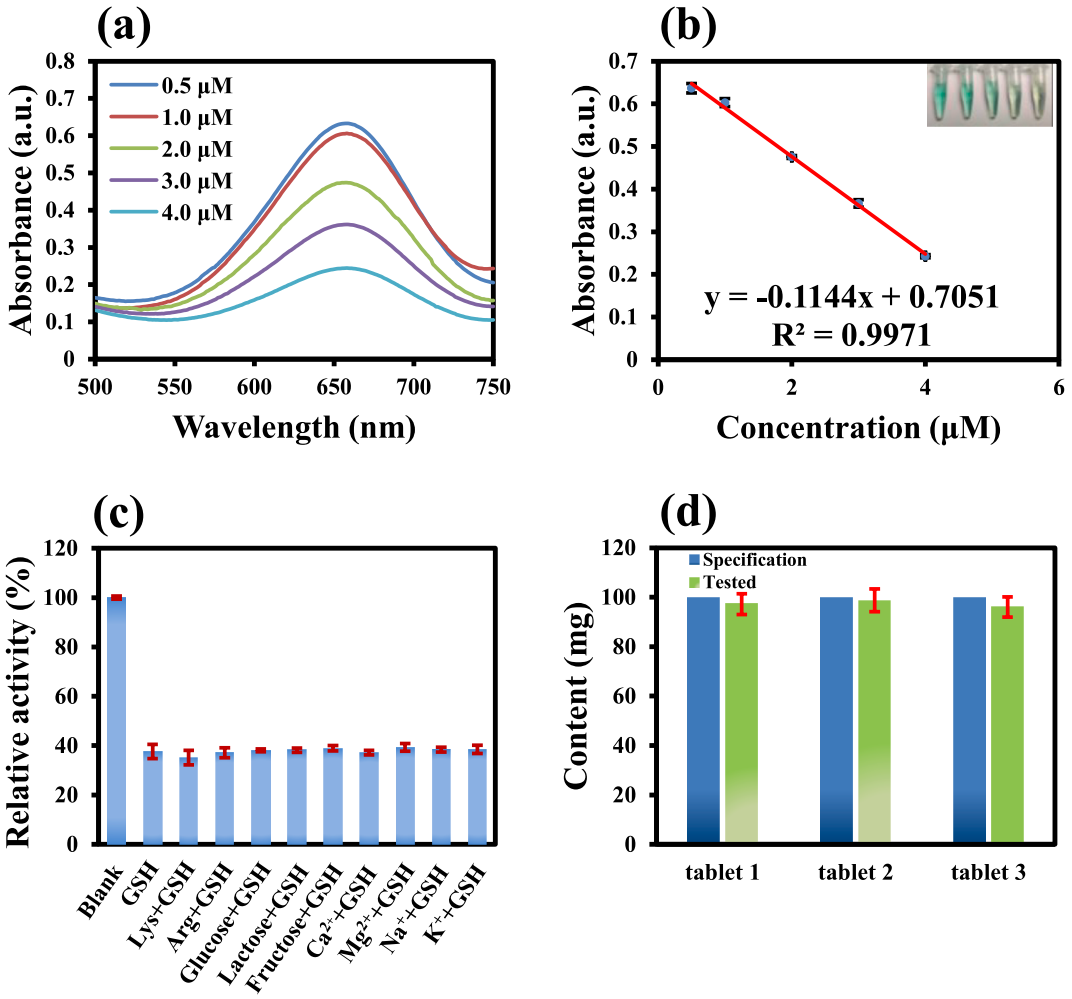

Fig. 6. (**a**) UV-Vis absorption spectra of Cu-ICA-oxidized TMB in the presence of different final concentrations GSH (0.5−4.0 μM); (**b**) calibration plots of the absorbance versus the final concentrations of GSH under the optimal conditions, inset: the corresponding digital photograph; (**c**) Selectivity study of the GSH colorimetric sensor through monitoring the absorbance at 658 nm of 4 μM of GSH (final concentrations) and 400 μM of interferences (final concentrations): Lys, Arg, glucose, lactose, fructose, K^{2+}, Mg^{2+}, Na^{+}, and Ca^{2+}; (**d**) Detection of GSH in commercial tablets (the specifications are used for comparison). The error bars represent the standard deviations of three independent measurements.

Table 2
Comparisons of colorimetric detection of GSH by different oxidase-like mimics.

Enzyme mimics	Liner range	LODs	Ref.
Fe-NC	1–10 μM	1.3 μM	[34]
Pt/NiCo-LDH NCs	50–500 mM	3.77 mM	[35]
COF-300-AR	1–15 μM	1 μM	[11]
Fe_3O_4 NPs	3–30 μM	3 μM	[36]
Pt NPs/COF-300-AR	4–4.0 μM	0.4 μM	[37]
D-ZIF-67	0.5–10 μM	0.2292 μM	[38]
Cu-ICA	0.5–4 μM	0.097 μM	This work

as the substrate, indicates that only a small quantity of TMB was required to reach the maximum catalytic activity.

Generally, hydroxyl radicals (•OH), singlet oxygen ($^1O_2$), and superoxide radicals (O_2^-) are the possible active species during the oxidation process. In this study, the radical trapping assay was performed to investigate the main active species in the catalytic reaction of Cu-ICA by introducing different radical scavengers. As depicted in Fig. 5c, with the increase in introducing amount of His and IPA, there exhibited an obvious decline in the relative activity of the Cu-ICA-catalyzed reaction. However, there was no apparent absorbance variance with the introduction of *p*-benzoquinone. Therefore, the $^1O_2$ and •OH may play the primary role in the catalytic process.

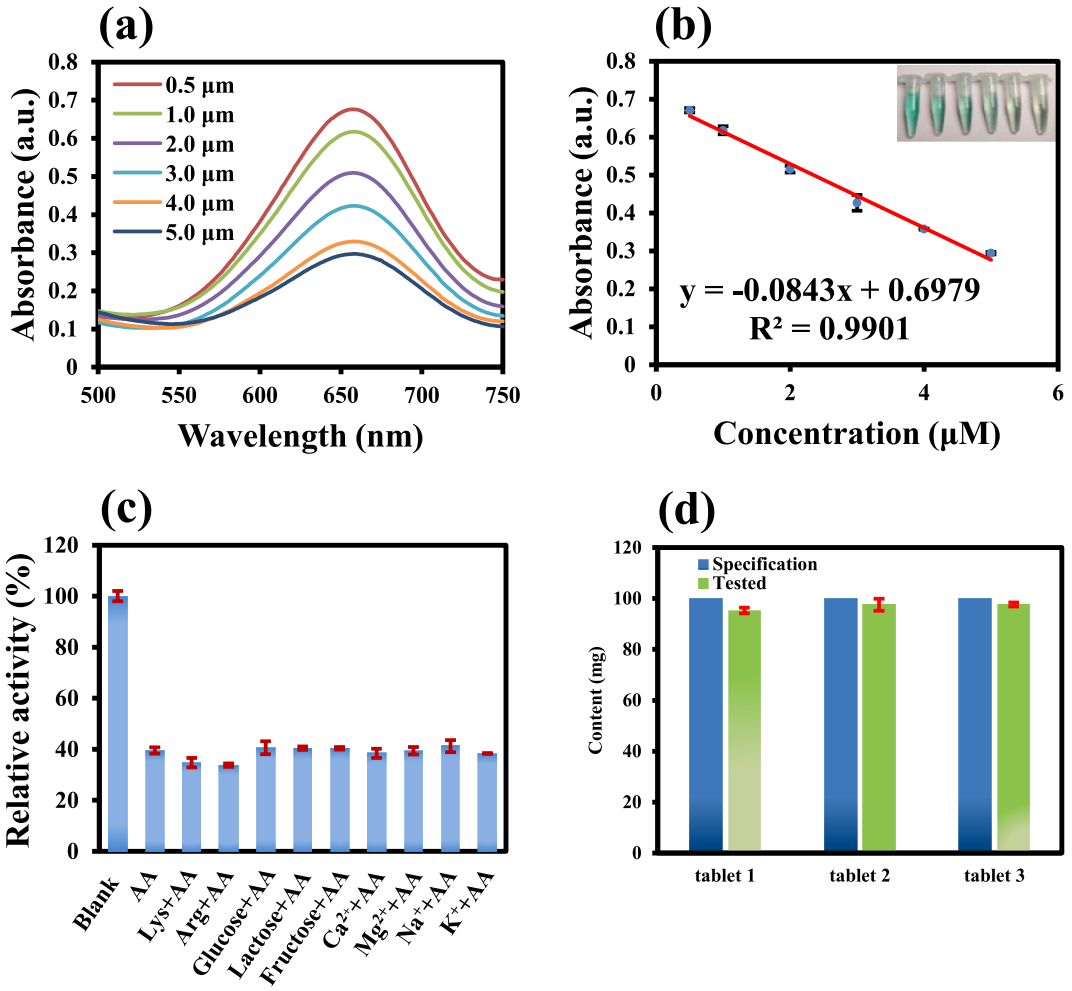

Fig. 7. (**a**) UV-Vis absorption spectra of Cu-ICA-oxidized TMB in the presence of at different final concentrations AA (0.5−5.0 μM); (**b**) calibration plots of the absorbance versus the concentrations of AA under the optimal conditions, inset: the corresponding digital photograph; (**c**) Selectivity study of the AA colorimetric sensor through monitoring the absorbance at 658 nm of 4 μM of AA (final concentrations) and 400 μM of interferences (final concentrations): Lys, Arg, glucose, lactose, fructose, K^{2+}, Mg^{2+}, Na^{+} and Ca^{2+}; (**d**) Detection of AA in commercial tablets (the specifications are used for comparison). The error bars represent the standard deviations of three independent measurements.

3.4. Colorimetric detection of GSH

As the most abundant intracellular nonprotein thiol, GSH plays a role in many cellular functions such as maintaining the intracellular redox activities. The GSH level is usually associated with several diseases, such as cardiovascular disease and cancer [33]. Therefore, it is significant importance to develop accurate and convenient methods for GSH detection. The Cu-ICA presented very good oxidase-like activity that can catalyze colorless TMB into blue ox-TMB. As a reducing agent, GSH can reduce the oxidation of TMB. Fig. 6a displays the absorbance at 658 nm of the reaction system with different concentrations of GSH. And depicted in Fig. 6b, in the final concentration range of 0.5–4 μM, GSH can reduce the blue oxidized TMB with a positive correlation linear relationship: $A = -0.1144\ [GSH] + 0.7051$, $R^2 = 0.9971$. The insert picture is the digital photograph, which can tentatively identify the concentration of GSH by visual recognition. Besides, the limit of detection (LOD) is calculated to be 0.097 μM. As compared with other oxidase mimics (Table 2), the analysis method based on Cu-ICA has a relatively low LOD and a wider detection range. As its shown in Fig. 6c, for some potential interfering substances, the absorbance value of the reaction system will hardly change, which indicates that there is a good selectivity in the detection of GSH. In addition, to further delve into the practicability of the developed method in real sample analysis, the GSH content in commercially available tablets was determined. As depicted in Fig. 6d, the GSH content determined by this method was in consistent with the sample specification, which indicate that the developed colorimetric detection method is suitable for the determination of GSH content in actual samples.

Table 3
Comparisons of colorimetric detection of AA by various oxidase-like mimics.

Enzyme mimics	Liner range	LODs	Ref.
Ce-MOF (MVCM)	20–500 μM	3.57 μM	[40]
CDs	1–30 μM	1.53 μM	[41]
MIL-53 (Fe)	28.6–190.5 μM	15 μM	[42]
Ce-BPyDC	1–20 μM	0.28 μM	[43]
FeMnzyme	8–56 μM	0.88 μM	[44]
Cu-ICA	0.5–5 μM	0.1304 μM	This work

3.5. Colorimetric detection of AA

AA, which is an important water-soluble antioxidant in human body [39], exerts an enormous function in maintaining human health. The deficiency of AA in human body will influence the synthesis of normal collagen and induce the disorders of cell connectivity, resulting in cardiovascular disease, anemia, scurvy, and weakened immunity, etc [32]. Therefore, it has attracted wide attentions of research in the detection of AA in biological and environmental samples. Fig. 7a shows the absorbance at 658 nm of the reaction system with different final concentrations of AA. Furthermore, Fig. 7b shows a linear relationship ($A = -0.0843$ [AA]+ 0.6979) of the absorbance at 658 nm versus AA final concentration in the range of 0.5–5 μM with $R^2 = 0.9901$, and LOD was 0.1304 μM. In Table 3, compared with other oxidase mimics, the analysis method based on Cu-ICA has a relatively low LOD and a wider detection range, indicate the high sensitivity of Cu-ICA for the AA detection. As displayed in Fig. 7c, for some potential interfering substances, the absorbance value of the reaction system was hardly changed, which indicates a good selectivity for the AA detection. In addition, to further evaluate the practicability of the developed method in real sample analysis, the AA content in commercially available tablets was determined. As depicted in Fig. 7d, the AA content determined by this method was in consistent with the sample specification. The results indicated that the Cu-ICA can act as a reliable functional material for AA detection.

4. Conclusions

In summary, an oxidase-like complex material, which takes ICA as the ligand and utilizes a fast one-pot synthesize strategy, was prepared and applied in the colorimetric detection of GSH and AA. The predominantly oxidase-like property of the Cu-ICA may be due to the abundant Cu active sites and the valence reduction of Cu. The hydration method of one-pot utilized to synthetic material suspension by one step shows the advantages of operating easily, reacting rapidly, detecting directly with uniform material dispersion. Furthermore, the synthesized Cu-ICA has excellent oxidase-like activity, and the v_{max} is much higher than the previously reported oxidase mimics. Moreover, the colorimetric sensing method based on Cu-ICA for the rapid detection (4 min) of GSH and AA shows excellent analytical performance and sensitivity. However, the K_m of Cu-ICA is large which means poor affinity to the reaction substrate. To solve this problem, the functional groups of the ICA can be further modified to improve the K_m of the enzyme mimics in the follow-up study.

Data availability statement

Data will be made available on request.

CRediT authorship contribution statement

Jia-Xin Li: Writing – original draft, Methodology, Investigation, Conceptualization. **Jia-Li Wang:** Methodology, Investigation. **Tong-Qing Chai:** Methodology, Investigation. **Feng-Qing Yang:** Writing – review & editing, Supervision, Resources, Project administration, Funding acquisition, Conceptualization.

Declaration of competing interest

The authors declare that they have no known competing financial interests or personal relationships that could have appeared to influence the work reported in this paper.

Acknowledgements

This work was supported by the National Key Research and Development Program of China (No. 2021YFC2103300).

Appendix A. Supplementary data

Supplementary data to this article can be found online at https://doi.org/10.1016/j.heliyon.2023.e22099.

References

[1] A. Arca-Ramos, G. Eibes, G. Feijoo, J.M. Lema, M.T. Moreira, Enzymatic reactors for the removal of recalcitrant compounds in wastewater, Biocatal. Biotransform. 36 (3) (2018) 195–215.

[2] Q. Husain, Potential applications of the oxidoreductive enzymes in the decolorization and detoxification of textile and other synthetic dyes from polluted water: a review, Crit. Rev. Biotechnol. 26 (4) (2006) 201–221.

[3] R. Jin, L. Zhao, X. Yan, X. Han, M. Liu, Y. Chen, Q. Li, D. Su, F. Liu, P. Sun, X. Liu, C. Wang, G. Lu, Lab in hydrogel portable kit: on-site monitoring of oxalate, Biosens. Bioelectron. 167 (2020), 112457.

[4] R. Bi, X. Ma, K. Miao, P. Ma, Q. Wang, Enzymatic biosensor based on dendritic gold nanostructure and enzyme precipitation coating for glucose sensing and detection, Enzym. Microb. Technol. 162 (2023), 110132.

[5] Y. Chong, Q. Liu, C. Ge, Advances in oxidase-mimicking nanozymes: classification, activity regulation and biomedical applications, Nano Today 37 (2021), 101076.

[6] Y. Lu, X. Zhang, Y. Huang, Tuning nanozyme property of Co@NC via V doping to construct colorimetric sensor array for quantifying and discriminating antioxidant phenolic compounds, Biosens. Bioelectron. 215 (2022), 114567.

[7] M. Feng, X. Li, X. Zhang, Y. Huang, Recent advances in the development and analytical applications of oxidase-like nanozymes, Trac. Trends Anal. Chem. 166 (2023), 117220.

[8] J. Tan, S.Y. Wu, Q.Q. Cai, Y. Wang, P. Zhang, Reversible regulation of enzymelike activity of molybdenum disulfide quantum dots for colorimetric pharmaceutical analysis, J. Pharm. Anal. 12 (1) (2022) 113–121.

[9] S.J. Yin, G.Y. Chen, C.Y. Zhang, J.L. Wang, F.Q. Yang, Zeolitic imidazolate frameworks as light-responsive oxidase-like mimics for the determination of adenosine triphosphate and discrimination of phenolic pollutants, Microchim. Acta 190 (1) (2023) 25.

[10] S.J. Yin, L.X. Li, F.Q. Yang, The light-responsive oxidase-like activity of MIL-125-NH2@Pd and its application in the determination of casein phosphopeptides, CrystEngComm 25 (2023) 2110–2118.

[11] P. Jin, X. Niu, F. Zhang, K. Dong, H. Dai, H. Zhang, W. Wang, H. Chen, X. Chen, Stable and reusable light-responsive reduced covalent organic framework (COF-300-AR) as a oxidase-mimicking catalyst for GSH detection in cell lysate, ACS Appl. Mater. Interfaces 12 (18) (2020) 20414–20422.

[12] Z. Li, F. Liu, Y. Jiang, P. Ni, C. Zhang, B. Wang, C. Chen, Y. Lu, Single-atom Pd catalysts as oxidase mimics with maximum atom utilization for colorimetric analysis, Nano Res. 15 (2022) 4411–4420.

[13] Z. Li, F. Liu, C. Chen, Y. Jiang, P. Ni, N. Song, Y. Hu, S. Xi, M. Liang, Y. Lu, Regulating the N coordination environment of Co single-atom nanozymes for highly efficient oxidase mimics, Nano Lett. 23 (2023) 1505–1513.

[14] N. Chaibakhsh, Z. Moradi-Shoeili, Enzyme mimetic activities of spinel substituted nanoferrites (MFe_2O_4): a review of synthesis, mechanism and potential applications, Mater. Sci. Eng., C 99 (2019) 1424–1447.

[15] X. Yang, M. Feng, X. Zhang, Y. Huang, Co, N, S co-doped hollow carbon with efficient oxidase-like activity for the detection of Hg^{2+} and Fe^{3+} ions, Microchem. J. 187 (2023), 108383.

[16] T.M. Simandi, L.I. Simandi, M. Gyor, A. Rockenbauer, A. Gomory, Kinetics and mechanism of the ferroxime (II)-catalysed biomimetic oxidation of 2-amino-phenol by dioxygen. A functional phenoxazinone synthase model, Dalton Trans. (7) (2004) 1056–1060.

[17] K. Jomova, M. Makova, S.Y. Alomar, S.H. Alwasel, E. Nepovimova, K. Kuca, C.J. Rhodes, M. Valko, Essential metals in health and disease, Chem. Biol. Interact. 367 (2022), 110173.

[18] A. De, M. Garai, H.R. Yadav, A.R. Choudhury, B. Biswas, Catalytic promiscuity of an iron (II)-phenanthroline complex, Appl. Organomet. Chem. 31 (1) (2017), e3551.

[19] X. Lai, Y. Shen, S. Gao, Y. Chen, Y. Cui, D. Ning, X. Ji, Z. Liu, L. Wang, The Mn-modified porphyrin metal-organic framework with enhanced oxidase-like activity for sensitively colorimetric detection of glutathione, Biosens. Bioelectron. 213 (2022), 114446.

[20] L. Zhang, Y. Hou, X. Guo, W. Liu, C. Lv, C. Zhang, Y. Jin, B. Li, Fe (III) bipyridyl or phenanthroline complexes with oxidase-like activity for sensitive colorimetric detection of glutathione, Luminescence 35 (8) (2020) 1350–1359.

[21] M.M. Ibrahim, A.M. Fathy, S.A. Al Harbi, A.E.M.M. Ramadan, Triazole based copper (II) complexes: synthesis, spectroscopic characterization, density function theory study, and biomimicking of copper containing oxidase proteins, J. Chin. Chem. Soc. 68 (8) (2021) 1496–1513.

[22] R. Wegner, M. Gottschaldt, H. Gorls, E.G. Jager, D. Klemm, Copper (II) complexes of aminocarbohydrate beta-ketoenaminic ligands: efficient catalysts in catechol oxidation, Chem. Eur J. 7 (10) (2001) 2143–2157.

[23] N.V. Loginova, T.Y.V. Koval Chuk, R.A. Zheldakova, N.P. Osipovich, V.L. Sorokin, G.I. Polozov, G.A. Ksendzova, G.K. Glushonok, A.A. Chernyavskaya, O. I. Shadyro, Synthesis and biological evaluation of copper (II) complexes of sterically hindered o-aminophenol derivatives as antimicrobial agents, Bioorg. Med. Chem. Lett. 16 (20) (2006) 5403–5407.

[24] S. Xu, H. Wu, S. Liu, P. Du, H. Wang, H. Yang, W. Xu, S. Chen, L. Song, J. Li, X. Shi, Z. Wang, A supramolecular metalloenzyme possessing robust oxidase-mimetic catalytic function, Nat. Commun. 14 (1) (2023).

[25] J. Wang, R. Huang, W. Qi, R. Su, Z. He, Construction of biomimetic nanozyme with high laccase- and catecholase-like activity for oxidation and detection of phenolic compounds, J. Hazard Mater. 429 (2022), 128404.

[26] B. Barszcz, T. Glowiak, J. Jezierska, Crystal and molecular structures of eight-coordinate (CuN_4O_4) and six-coordinate (CuN_4O_4) Cu (II) complexes with 4-methyl-5-imidazole-carboxaldehyde or 1-benzyl-2-hydroxymethylimidazole, respectively: spectroscopic and potentiometric studies, Polyhedron 18 (1999) 3713–3721.

[27] Y. Zhong, Q. Li, M. Lu, T. Wang, H. Yang, Q. He, X. Cui, X. Li, S. Zhao, A colorimetric sensing strategy based on enzyme@metal-organic framework and oxidase-like IrO_2/MnO_2 nanocomposite for alpha-glucosidase inhibitor screening, Mikrochim. Acta 187 (12) (2020).

[28] M.H. Sorouraddin, K. Amini, A. Naseri, J. Vallipour, J. Hanaee, M.R. Rashidi, A new multi-wavelength model-based method for determination of enzyme kinetic parameters, J. Biosci. 35 (3) (2010) 395–403.

[29] M. Cui, Y. Zhao, C. Wang, Q. Song, The oxidase-like activity of iridium nanoparticles, and their application to colorimetric determination of dissolved oxygen, Mikrochim. Acta 184 (9) (2017) 3113–3119.

[30] J. Wang, Y. Wang, D. Zhang, C. Chen, Intrinsic oxidase-like nanoenzyme Co_4S_3/Co $(OH)_2$ hybrid nanotubes with broad-spectrum antibacterial activity, Acs Appl. Mater. Interfaces (2020).

[31] W. Lu, J. Chen, L. Kong, F. Zhu, Z. Feng, J. Zhan, Oxygen vacancies modulation Mn_3O_4 nanozyme with enhanced oxidase-mimicking performance for L-cysteine detection, Sens. Actuators B Chem. 333 (2021), 129560.

[32] J. Wan, J. Zou, S. Zhou, F. Pan, F. Hua, Y. Zhang, J. Nie, Y. Zhang, A bimetallic (Ni/Co) metal–organic framework with excellent oxidase-like activity for colorimetric sensing of ascorbic acid, Anal. Methods 15 (14) (2023) 1819–1825.

[33] H.S. Jung, X. Chen, J.S. Kim, J. Yoon, Recent progress in luminescent and colorimetric chemosensors for detection of thiols, Chem. Soc. Rev. 42 (14) (2013) 619–631.

[34] Y. Gu, Z. Cao, M. Zhao, Y. Xu, N. Lu, Single-atom Fe nanozyme with enhanced oxidase-like activity for the colorimetric detection of ascorbic acid and glutathione, Biosensors 13 (4) (2023) 487.

[35] X. Cao, H. Yang, Q. Wei, Y. Yang, M. Liu, Q. Liu, X. Zhang, Fast colorimetric sensing of H_2O_2 and glutathione based on Pt deposited on NiCo layered double hydroxide with double peroxidase-/oxidase-like activity, Inorg. Chem. Commun. 123 (2021), 108331.

[36] Y. Ma, Z. Zhang, C. Ren, G. Liu, X. Chen, A novel colorimetric determination of reduced glutathione in A549 cells based on Fe_3O_4 magnetic nanoparticles as peroxidase mimetics, Analyst (London) 137 (2) (2012) 485–489.

[37] P. Jin, X. Niu, Z. Gao, X. Xue, F. Zhang, W. Cheng, C. Ren, H. Du, A. Manyande, H. Chen, Ultrafine platinum nanoparticles supported on covalent organic frameworks as stable and reusable oxidase-like catalysts for cellular glutathione detection, ACS Appl. Nano Mater. 4 (6) (2021) 5834–5841.

[38] M. Han, M. Ren, Z. Li, L. Qu, L. Yu, A two-dimensional thin Co-MOF nanosheet as a nanozyme with high oxidase-like activity for GSH detection, New J. Chem. 46 (22) (2022) 10682–10689.
[39] A. Wu, H. Ding, W. Zhang, H. Rao, L. Wang, Y. Chen, C. Lu, X. Wang, A colorimetric and fluorescence turn-on probe for the detection of ascorbic acid in living cells and beverages, Food Chem. 363 (2021), 130325.
[40] M. Fu, F. Xu, J. Yan, C. Wang, G. Fan, G. Song, B. Chai, Mixed valence state cerium metal organic framework with prominent oxidase-mimicking activity for ascorbic acid detection: mechanism and performance, Colloids Surf. A Physicochem. Eng. Asp. 641 (2022), 128610.
[41] J. Li, Y. Zhou, Y. Xiao, S. Cai, C. Huang, S. Guo, Y. Sun, R. Song, Z. Li, Carbon dots as light-responsive oxidase-like nanozyme for colorimetric detection of total antioxidant capacity in fruits, Food Chem. 405 (2023), 134749.
[42] L. Ai, L. Li, C. Zhang, J. Fu, J. Jiang, MIL-53(Fe): a metal-organic framework with intrinsic peroxidase-like catalytic activity for colorimetric biosensing, Chem. Eur J. 19 (45) (2013) 15105–15108.
[43] L. Luo, L. Huang, X. Liu, W. Zhang, X. Yao, L. Dou, X. Zhang, Y. Nian, J. Sun, J. Wang, Mixed-valence Ce-BPyDC metal–organic framework with dual enzyme-like activities for colorimetric biosensing, Inorg. Chem. 58 (17) (2019) 11382–11388.
[44] Y. Han, L. Luo, L. Zhang, Y. Kang, H. Sun, J. Dan, J. Sun, W. Zhang, T. Yue, J. Wang, Oxidase-like Fe–Mn bimetallic nanozymes for colorimetric detection of ascorbic acid in kiwi fruit, Lebensm. Wiss. Technol. 154 (2022), 112821.